

blood

Prepublished online Jun 8, 2009;
doi:10.1182/blood-2009-03-213934

Successful treatment of the murine model of cystinosis using bone marrow cell transplantation

Kimberly Syres, Frank Harrison, Matthew Tadlock, James V. Jester, Jennifer Simpson, Subhojit Roy, Daniel R. Salomon and Stephanie Cherqui

Information about reproducing this article in parts or in its entirety may be found online at:
http://bloodjournal.hematologylibrary.org/misc/rights.dtl#repub_requests

Information about ordering reprints may be found online at:
<http://bloodjournal.hematologylibrary.org/misc/rights.dtl#reprints>

Information about subscriptions and ASH membership may be found online at:
<http://bloodjournal.hematologylibrary.org/subscriptions/index.dtl>



Successful treatment of the murine model of cystinosis using bone marrow cell transplantation

***Running title:* Bone marrow transplants for cystinosis**

Kimberly Syres*, Frank Harrison*, Matthew Tadlock*, James V. Jester[†], Jennifer Simpson[†], Subhojit Roy[‡], Daniel R. Salomon*, and Stephanie Cherqui*[§]

*The Scripps Research Institute, Department of Molecular and Experimental Medicine, 10550 North Torrey Pines Road, La Jolla, California 92037, USA.

[†]University of California Irvine, Department of Ophthalmology, 101 The City Drive, Orange, California 92868, USA.

[‡]University of California San Diego, Department of Neurosciences, 9500 Gilman Drive, La Jolla, California 92037, USA.

[§]Corresponding author: Stephanie Cherqui, Ph.D.
Department of Molecular and Experimental Medicine
The Scripps Research Institute, 10550 North Torrey Pines Road,
La Jolla, California 92037, USA.
Phone: 858 784 2734
Fax: 858 784 2121
scherqui@scripps.edu

Abstract

Cystinosis is an autosomal recessive metabolic disease that belongs to the family of lysosomal storage disorders. The defective gene is *CTNS* encoding the lysosomal cystine transporter, cystinosin. Cystine accumulates in every organ in the body and leads to organ damage and dysfunction including renal defects. Using the murine model for cystinosis, *Ctns*^{-/-} mice, we performed syngeneic bone marrow cell (BMC), hematopoietic stem cell transplantation (HSC) and mesenchymal stem cell (MSC) transplantation. Organ-specific cystine content was reduced by 57% to 94% in all organs tested in the BMC-treated mice. Confocal microscopy and quantitative-PCR revealed a large quantity of transplanted BMC in all organs tested, from 5% to 19% of the total cells. Most of these cells were not from the lymphoid lineage, but part of the intrinsic structure of the organ. The natural progression of renal dysfunction was prevented and deposition of corneal cystine crystals was significantly improved in the BMC-treated mice. HSC had the same therapeutic effect as whole BMC. In contrast, MSC did not integrate efficiently in any organ. This work is a proof of concept for using HSC transplantation as a therapy for cystinosis and highlights the efficiency of this strategy for a chronic, progressive degenerative disease.

Introduction

Cystinosis is an autosomal metabolic hereditary disease characterized clinically by generalized proximal renal tubular dysfunction (Fanconi syndrome) and biochemically by lysosomal accumulation of cystine, which leads to the formation of cystine crystals. Cystinosis belongs to the family of lysosomal storage disorders (LSD) characterized by the tissue accumulation of incompletely degraded substrates leading to multiple organ dysfunction. The gene underlying cystinosis, *CTNS*, encodes a 7 transmembrane domain protein, cystinosin¹, a lysosomal cystine transporter^{2,3}. Affected individuals typically present before two years old with symptoms of severe fluid and electrolyte disturbances (i.e. dehydration, vomiting, poor growth, rickets). Without specific treatment they progress to end-stage renal failure by the end of the first decade⁴; in the United States, cystinosis accounts for approximately 1.4% of children on dialysis and 2% of pediatric kidney transplants (North American Pediatric Renal Trials and Collaborative Studies, 2008 annual report). Cystine accumulation eventually leads to multi-organ dysfunction and patients present with photophobia and blindness, hypothyroidism, hypogonadism, diabetes, myopathy and central nervous system defects⁵.

Different treatments have been tested for LSD including enzyme replacement, substrate depletion and bone marrow transplantation⁶. For cystinosis, substrate depletion with the drug cysteamine reduces the intracellular concentration of cystine. If used early in the disease and in high doses, it can reduce the subsequent progression of renal glomerular damage and other defects⁷. However, the need for frequent dosing and multiple undesirable side effects such as digestive intolerance and persistent odor, render

its chronic administration difficult. Moreover, the proximal renal tubulopathy is not sensitive to cysteamine.

Over the past two decades, a number of reports have established a proof of principle for allogeneic bone marrow stem cell transplantation in several LSD including Hurler disease (MPS-I), globoid-cell leukodystrophy (GLB; Krabbe disease) and adrenoleukodystrophy^{8,9}. Treatment of Hurler patients performed before the age of two, has been the most gratifying, and the reconstitution of enzymatic activity is correlated with prolonged survival and in some cases, normal or near normal cognitive development and myocardial function^{8,10-12}.

Cystinosin is a lysosomal transmembrane protein that cannot be secreted. Therefore, in contrast to Hurler syndrome, the normal enzyme produced by tissue-engrafted cells cannot spread to be recaptured by other cells lacking a functional *Ctns* gene. Therefore, a proof of concept for bone marrow cell transplantation as a therapy for cystinosis is necessary. We used the mouse model, *Ctns*^{-/-} mice, which accumulate cystine and cystine crystals in all organs tested¹³. *Ctns*^{-/-} mice develop ocular changes similar to those observed in affected patients, bone and muscular defects and behavioral anomalies. *Ctns*^{-/-} mice backcrossed on a C57BL/6 background develop an incomplete proximal tubulopathy and renal failure by 15 months of age¹⁴.

Here we report that syngeneic bone marrow transplantation from wildtype donors into *Ctns*^{-/-} mice successfully protected these animals from the progression of the kidney tissue injury and corneal cystine deposition that represent two of the major clinical problems faced by children and young adults with this genetic disorder. There was significant engraftment of donor bone marrow-derived cells in every tissue compartment

tested as determined by confocal microscopy and quantitative PCR. Mechanistically, only engraftment of bone marrow cells producing a functional *Ctns* was able to reverse the disease process. Second, quantitative expression of functional *Ctns* and tissue colonization by BMC-derived cells measured by luciferase imaging in these animals correlated in each tissue compartment with reduction of cystine levels of 57% to 94% as measured by tandem mass spectrometry.

Materials and Methods

Mice. C57BL/6 *Ctms*^{-/-} mice were provided by Dr. Antignac (Inserm U574, Paris, France) and bred continuously at The Scripps Research Institute. Transgenic mice constitutively expressing GFP (C57BL/6-Tg(ACTB-EGFP)10sb/J, Jackson Laboratory, Bar Harbor, MI) were obtained from The Jackson Laboratory. Transgenic mice constitutively expressing firefly luciferase were provided by Dr. Geusz (Bowling Green State University, Bowling Green, OH). All protocols were approved by the AAALAC-Accredited Institutional Animal Care and Use Committee of The Scripps Research Institute.

BMC and HSC isolation, MSC generation and cell transplantation. BMC were flushed from the long bones of 6-8 week old mice and transplanted without further culture or processing. Sca1⁺ bone marrow progenitors (HSC) were sorted using anti-Sca1 antibody conjugated to mini-magnetic beads (Miltenyi Biotec, Auburn, CA). MSC were generated as previously described¹⁵. Briefly, BMC from GFP-transgenic mice were plated at a density of 5 x 10⁶ cells per milliliter in DMEM-low glucose-containing 10% fetal bovine serum (Hyclone, Logan, UT), 3.7 g/l sodium bicarbonate, 10 mM HEPES and 100 u/ml penicillin/streptomycin (Gibco Invitrogen, Carlsbad, CA)). Cultures were plated 3.5 ml per well of 6-well tissue culture dishes and were kept at 37°C 5%CO₂. The media was changed 72 h post-plating and then every 3 days. When cultures reached confluence, cells were split at a 1:2 ratio. At each passage, cells were stained with phycoerythrin-conjugated anti-CD45, CD44 (BD Pharmingen, San Jose, CA), CD34, CD31 (Caltag Invitrogen, Burlingame, CA), CD105 (R&D Systems, Minneapolis, MN)

and CD90.2 (eBioscience, San Diego, CA) antibodies and analyzed by flow cytometry to determine the phenotype of the cells. Cells were injected via the tail vein. The mice were lethally (cesium radiation, 8 Gy) for BMC and HSC, or sub-lethally (3.6 Gy) for MSC, irradiated the day preceding the injection. To analyze engraftment, fresh blood was treated with red blood cell lysis buffer (eBioscience) and subjected to flow cytometry to quantify GFP-positive cells. Lineage-specific staining and flow cytometry allowed determination of the hematopoietic chimerism for T cells (Cy-chrome-conjugated anti-CD3epsilon, Pharmingen), B cells (Phycoerythrin (PE)-conjugated anti-CD19, BioLegend, San Diego, CA), and macrophages (PE-conjugated MAC3, Pharmingen). Appropriate isotype controls were used for each.

Blood and urine analysis. Serum was obtained by eye bleeds and 24 h urine collections were done in metabolic cages. Serum and urine phosphate levels as well as serum creatinine, urea, and alkaline phosphatase were estimated by using colorimetric assays according to the manufacturer recommendations (BioAssay Systems, Hayward, CA). Protein levels in urine were measured using Pierce BCA Protein Assay Kit (Rockford, IL).

RT-qPCR. RNA was isolated from explanted tissues by homogenization in 750 μ l Trizol LS Reagent (Invitrogen). Phase separation was performed with the addition of 200 μ l chloroform followed by centrifugation. After removal of the aqueous phase, RNA was recovered by precipitation with isopropyl alcohol. RNA was purified using the RNeasy mini-protocol for RNA cleanup including DNase treatment on column (Qiagen, Valencia,

CA). 1 µg of RNA for each tissue was reverse transcribed using iScript cDNA Synthesis Kit (Bio-Rad, Hercules, CA). For peripheral blood engraftment determination, 300µl of mouse whole blood was collected by cardiac puncture and placed in 600µl PAXgene blood RNA preservative solution obtained from PAXgene Blood RNA Tubes (PreAnalytix Qiagen) followed by RNA purification using the PAXgene Blood RNA Kit (PreAnalytix Qiagen).

Ctms-specific qPCR was performed using 2 µl of cDNA and 2x Universal TAQ man master mix (Roche Diagnostics, Indianapolis, IN), *Ctms* primer mix (in *Ctms* exon 8: *Ctms* oligo 1: TTGTGGCTGCAGTCGGTATC, *Ctms* oligo 2: AGCTTGATGTAGGAGAAGCAGAAGA, and *Ctms* probe: CACATGGCTCCAGTTC (Applied Biosystems, Foster City, CA) and 18s primer mix (Applied Biosystems) on an Applied Biosystems 7900 HT.

Immunofluorescence analysis. Tissues were fixed in formaldehyde 5%, equilibrated in sucrose 20% overnight and frozen in Tissue-Tek Optimal Cutting Temperature buffer at -80°C (Sakura Finetek U.S.A, Torrance, CA). 12 to 20 µm sections were cut and blocked with 1% BSA, 10% donkey serum in PBS. The blocking buffer was then diluted 1:5 in PBS and antibody added in the dilutions denoted below and incubated with sections at room temperature for 1 hour; the lectins were incubated for 2 hours. Each tissue was stained with DAPI and Bodipy-Phalloidin (1:500 dilutions for 30 min, Molecular Probes, Eugene, OR) or Cy5-conjugated anti-F4/80 antibody (1:50 dilution, Serotec) and biotinylated anti-mouse CD45 antibody (1:500 dilution, BD Pharmingen) followed by Alexa 594-conjugated streptavidin (1:100 dilution, Invitrogen). Kidney sections were

stained with Rhodamine-conjugated Dolichos Biflorus Agglutinin (1:100 dilution), Rhodamine-conjugated Ricinus Communis Agglutinin I (1:250 dilution), biotinylated Lotus Tetragonolobus lectin (1:100 dilution) (Vector Laboratories, Burlingame, CA) followed by Alexa 594-conjugated streptavidin, and rabbit anti-human von Willebrand Factor (vWF, 1:200 dilution, Dako, Carpinteria, CA) followed by donkey anti-rabbit IgG conjugated with Cy5 (1:100 dilution). Brain sections were stained with a mouse pan anti-axonal microfilament antibody (1:250 dilution, Covance, Emeryville, CA) and a mouse anti-glial fibrillary acidic protein (1:500 dilution, Millipore, Billerica, MA), followed by a donkey anti-mouse IgG conjugated with Alexa-594 (1:100 dilution, Jackson ImmunoResearch, West Grove, PA). Images were acquired using a Rainbow Radiance 2100 Laser Scanning Confocal system attached to a Nikon TE2000-U inverted microscope (BioRad-Carl Zeiss, Thornwood, NY). All images were 8-bit optical image slices (0.5 μm interval step slices) acquired using LaserSharp 2000 software. Images were then analyzed with IMARIS 4.2 imaging software (Bitplane Scientific Solutions, Saint Paul, MN) to generate 3-D reconstruction series of optical slices (Z-stacks).

Tandem scanning reflectance confocal microscopy. Reflectance confocal microscopy was performed on enucleated mouse eyes of various ages. Examinations were performed using a Tandem Scanning Confocal Microscope (TSCM, Tandem Scanning Corporation, Reston, VA) with a 24x surface-contact objective (numerical aperture, 0.6; working distance, 1.5 mm), Oriel 18011 Encoder Mike Controller (Oriel Corp., Stratford, CT) for focal plane control, and Dage MTI VE-1000 camera (Dage MTI, Michigan City, IN). One drop of artificial tear solution was placed on the tip of the objective as a coupling

gel. All camera settings were kept constant throughout the experiment. For each examination, repeated through-focus data sets were obtained from the peripheral cornea and limbal region to identify cystine crystals and GFP-positive cells.

Cystine content measurement. Explanted tissues were grounded in 500 μ l of N-Ethylmaleimide (Fluka Biochemika, Bushs, Switzerland) at 650 μ g/ml for cystine measurements. The proteins were precipitated using 15% 5-sulfosalicylic acid dihydrate (Fluka Biochemika), resuspended in NaOH 0.1N and measured using the Pierce BCA protein assay kit. The cystine-containing supernatants were sent to the UCSD Biochemical Genetics laboratory for measurements by mass spectrometry.

Live animal luciferase imaging. Mice transplanted with BMC isolated from luciferase transgenic mice were measured at 2, 3 and 4 months post-transplantation using the IVIS Imaging System 200 Series (Caliper Life Sciences, Hopkinton, MA). First, the mice were anesthetized and 75 μ l of luciferin (30 mg/ml, Caliper Life Sciences) was injected intraperitoneally 10 min prior to the observation. Quantitative signal analysis was done using the Living Image 2.5 software (Caliper Life Sciences).

Statistics. We expressed data as arithmetic means \pm s.d. and performed statistical analysis using one-tailed t tests as the samples were large enough and normally distributed, $P < 0.05$ was considered as statistically significant. Corneal cystine crystals were recorded as a simple present or absent result and statistics were done by Chi Square.

Results

Freshly harvested BMC were used for transplantation. MSC were prepared by culture following Dr. Merelilles' protocol¹⁵ and used at passage 20. The phenotype of the MSC were tested and confirmed by flow cytometry at the time of transplantation: positive for CD44, CD90.2, CD105 and negative for CD45, CD31, CD34 (data not shown). We transplanted 2×10^7 wildtype C57BL/6 BMC (WT BMC) or 10^6 MSC in lethally or sub-lethally irradiated *Ctns*^{-/-} mice, respectively. As controls, we transplanted 2×10^7 *Ctns*^{-/-} BMC into lethally irradiated *Ctns*^{-/-} mice. The groups were: wildtype mice, untreated *Ctns*^{-/-} mice, WT BMC-treated *Ctns*^{-/-} mice and *Ctns*^{-/-} BMC-treated *Ctns*^{-/-} mice. Within each group the animals were age-matched littermates and a mix of males and females. Mice were between 2 and 4 months old when transplanted and sacrificed 4 months later for analysis. These experiments were repeated three times (n=5 mice) for a total of 15 mice per group. Three mice per group were sacrificed 2 months post-injection to determine if tissue integration was increasing with time. To allow tracking of cells by confocal microscopy, we transplanted 4 *Ctns*^{-/-} mice and 4 wildtype controls with BMC from GFP transgenic mice. All transplanted MSC were from GFP transgenic mice.

Cell engraftment was determined in peripheral blood by quantifying either GFP-positive cells by flow cytometry or by RT-qPCR for the wildtype *Ctns* gene. Engraftment ranged from 5 to 90% in mice transplanted with WT BMC and 3 to 6% in mice transplanted with MSC. The survival rate for BMC-transplanted mice after lethal irradiation was 93% and all the surviving mice exhibited benefits. The contribution of donor-derived cells within each lineage was determined for 5 mice transplanted with GFP-transgenic BMC and for which the peripheral blood engraftment was $72 \pm 17\%$;

86±7% were GFP-positive T-lymphocytes, 69±11% B-lymphocytes and 45±21% were macrophages.

Kidney

In all the experimental groups described above, renal function was assessed by measuring creatinine, urea, alkaline phosphatase, and phosphate levels in the serum and creatinine clearance, protein and phosphate in 24-hour urine collections. Serum creatinine and urea of *Ctns*^{-/-} mice transplanted with WT BMC was significantly better than control *Ctns*^{-/-} mice and *Ctns*^{-/-} mice transplanted with *Ctns*^{-/-} BMC (Table 1). Moreover, kidney function of mice transplanted with WT BMC was not significantly different than wildtype controls. Serum urea was increased in *Ctns*^{-/-} mice treated with wildtype MSC compared to *Ctns*^{-/-} mice treated with WT BMC, but the creatinine levels were normal.

Kidney sections for each group of mice defined above were analyzed by confocal microscopy for the presence of GFP-positive cells. We did not observe any GFP-positive cells in *Ctns*^{-/-} mice treated with *Ctns*^{-/-} BMC (Figure 1A and 1B) as a negative control for imaging of GFP in the experimental groups. Only few GFP-positive cells were observed in mice transplanted with GFP MSC (less than 5 cells per section; data not shown). Wildtype mice treated with WT BMC isolated from GFP transgenic mice (GFP BMC) also revealed very few GFP-positive cells in the kidney (Figure 1C and 1D). In contrast, *Ctns*^{-/-} mice transplanted with GFP BMC showed abundant BMC-derived cells (Figure 1E and 1F).

Most of the GFP-positive cells in *Ctns*^{-/-} mice transplanted with GFP BMC were interstitial but only a few were of lymphoid or macrophage lineage as defined by CD45

and F4/80 staining, respectively (Figure 2A). GFP-positive cells co-localized with proximal and distal tubular cells and some were in glomeruli (Figure 2B, 2C, 2D). Finally, GFP-positive cells were co-localized to tubular and glomerular basement membranes or with endothelial cells (Figure 2E and 2F).

Eye and brain

One eye per mouse was analyzed by confocal microscopy for the presence or absence of corneal cystine crystals and GFP-positive cells. Cystine crystals were detected only in mice over 7 months old. Out of 7 *Ctns*^{-/-} BMC-treated *Ctns*^{-/-} mice, 6 presented cystine crystals (Figure 3D). However, in 7 age-matched WT BMC-treated mice, only 3 had cystine crystals in the cornea (treated vs. non-treated $P < 0.05$; Chi Square). GFP-positive cells were observed in the peripheral cornea, localized to the corneal stroma (Figure 3A) and adjacent to the basal cells of the corneal epithelium (Figure 3B). GFP-positive cells generally had a dendritic (Langerhans) cell-like morphology. At the vascularized limbus, a heavy peri-vascular infiltrate was also observed (Figure 3C). No GFP-positive cells were observed in mice transplanted with GFP MSC.

We analyzed the brains by confocal microscopy. GFP-positive cells were observed in all brain regions. Most of these cells were associated with blood vessels. Some were small, round and were associated with delicate intraparenchymal vessels. These cells were particularly prominent in the basal ganglia and thalamus and were found within the blood vessel lumens. Some also appeared to be attached to the endothelium and some large, flattened GFP positive cells were also seen. These cells with an endothelial-like morphology were further characterized by double immunofluorescence

staining; they were positive for smooth muscle or endothelial markers (Figure 3E and 3F). A few cells also co-localized with macrophage and glial markers (Figure 3G and 3H). No GFP-positive cells were observed in mice transplanted with MSC.

Muscle, spleen, liver and heart

Mice transplanted with MSC present with very few GFP-positive cells in muscle, spleen, liver and heart. In contrast, mice that received BMC had a large quantity of transplanted BMC-derived cells in all these tissues. In the muscle, most of the GFP-positive cells were non-lymphoid lineage interstitial cells. However, the observation of some GFP-positive muscle cells indicated a subset of transplanted BMC-derived cells probably fused with muscle fibers (Figure 4A-C). In the heart, the GFP-positive cells were interstitial (data not shown). In the liver, most of the GFP-positive cells were Kupffer cells, co-localizing with macrophages (F4/80) and leukocyte lineage cells (CD45-positive; data not shown). Spleen demonstrated the most GFP-positive cells of any tissue. Surprisingly, the majority was not of the lymphoid lineage (CD45 and F4/80 negative) but they were vWF and f-actin-positive consistent with splenic reticulo-endothelial cells (Figure 4D-F).

Cystine content, tissue *Ctns* expression and dynamics

Cystine contents of brain, eye, heart, kidney, liver, muscle, and spleen was measured at 2 months (n=3/group) and 4 months (n=12/group) (Table 2 and Figure 5). Cystine levels increased in all tissues in *Ctns*^{-/-} BMC-treated mice as a function of time. In MSC-treated mice, a decrease in cystine level was significant only in heart at 2 months

but levels increased at 4 months. In contrast, as early as 2 months, *Ctns*^{-/-} mice transplanted with WT BMC demonstrated a decrease in cystine content compared to *Ctns*^{-/-} BMC-treated mice. This cystine content decrease was observed in all the tissues except the kidney, but was only statistically significant in the spleen and liver. By 4 months, cystine levels were significantly less in WT BMC-treated mice in all the tissues tested ranging between a 57% decrease in the brain to 94% in the liver.

RT-qPCR with *Ctns*-specific primers was performed in the same tissues at 2 and 4 months post-transplant (Table 3). No *Ctns* expression was detected in *Ctns*^{-/-} BMC-treated mice. The results confirmed the high level of engraftment observed for WT BMC and the low engraftment of MSC-derived cells. Thus, *Ctns* expression decreased in MSC-treated mice in all tissues except spleen between 2 and 4 months. *Ctns* expression was highest in mice treated with WT BMC in the spleen, confirming the confocal microscopy data (Figure 4). To show the changes in time, we normalized the RT-qPCR values for *Ctns* expression at 2 and 4 months by taking the ratio of the wildtype values to the *Ctns*^{-/-} mice transplanted with WT BMC. These results demonstrate that *Ctns* expression increased between 2 and 4 months post-injection in every tissue (Figure 6B). By 4 months *Ctns* expression ranged between 5.4% of the total *Ctns* expressed in wildtype mice in muscle to 19.3% in spleen.

Finally, to follow the fate of transplanted BMC expressing a functional *Ctns* gene in live animals as a function of time, we transplanted 10 *Ctns*^{-/-} mice and 5 wildtype controls with BMC isolated from luciferase-transgenic mice. The mice were imaged at 2, 3 and 4 months post-transplant and luciferase expression was quantitatively measured. At each time point, four pictures for each mouse are taken representing the ventral, dorsal,

left and right side views. Figure 6A is a representative ventral view picture of the same *Ctns*^{-/-} and wildtype mice at the three different time points. The significant increase of luciferase intensity and tissue area with time is clearly evident in the *Ctns*^{-/-} mouse and correlates with our evidence for the engraftment of BMC-derived cells in multiple tissues. In contrast, in wildtype mice the luciferase expression remains minimal over time.

Hematopoietic stem cells

We showed that whole BMC efficiently integrated in multiple organs resulting in significant decreases of cystine content in these tissues. BMC is a heterogeneous mixture of cells that contains a small number of HSC. For the purpose of a clinical application, we need to know if whole bone marrow is necessary to achieve our objectives or if similar results can be obtained with purified HSC only. We lethally irradiated and transplanted 10 two-month old *Ctns*^{-/-} mice with Sca1⁺ HSC isolated from GFP-transgenic mice. These were all sacrificed at 4 months post-transplantation for analysis. All these mice had high levels of peripheral blood engraftment of transplanted cells, ranging from 73% to 94% (hematopoietic lineage chimerism: 95±3% for T-lymphocytes, 65±14% for B-lymphocytes and 50±14% for macrophages). Controls included non-treated *Ctns*^{-/-} mice and wildtype animals at the same ages. Mice transplanted with Sca1⁺ GFP HSC showed abundant GFP-positive cells within all the tissues tested by confocal microscopy (data not shown). RT-qPCR with *Ctns*-specific primers showed a high level of engraftment of Sca1⁺ HSC-derived cells in all the tissues tested of *Ctns*^{-/-} treated mice (Table 4a). The relative expression of *Ctns* gene in HSC-treated *Ctns*^{-/-} mice compared to

wildtype was expressed in percentages, between 2.1% in the brain to 77.5% in the spleen. Tissue cystine levels were also significantly decreased in HSC-treated *Ctns*^{-/-} mice compared to non-treated *Ctns*^{-/-} mice controls, between a 43.5% decrease in the kidney to 93.2% in the liver (Table 4b). The renal function of HSC-transplanted *Ctns*^{-/-} mice was also normal as defined by serum urea and creatinine levels (data not shown).

Discussion

Cystinosis is a hereditary, autosomal recessive genetic disease of childhood that results in progressive cellular injury to many different tissues due to the accumulation of cystine in lysosomes. The introduction of oral cysteamine therapy in 1994¹⁶ has significantly improved the quality of life of patients with cystinosis and has reduced the rate of progression of tissue injury⁷. However, curative therapy for hereditary genetic diseases like the lysosomal storage disorders (LSD) requires the addition of the gene to many cells, typically in multiple tissue compartments, or the progressive replacement of injured and dying cells by cells expressing the functional version of the gene. Recently, an attempt to deliver the *CTNS* gene to the liver of *Ctns*^{-/-} mice with an adenoviral-vector demonstrated a limited decrease in cystine content but only with young animals and very low expression of the transgene¹⁴. Stem cell transplantation represents an alternative strategy and there has been some success in other LSD, particularly with Hurler disease^{8,9}. Here we report the effective use of both BMC and HSC transplantation to prevent the development and progression of kidney injury and dysfunction in *Ctns*^{-/-} mice. We also demonstrate the engraftment of BMC- and HSC-derived cells in multiple tissue compartments known to reflect clinical disease in the course of cystinosis and document significant reductions in tissue cystine content in all these compartments.

The therapeutic potential of stem cell transplantation for renal disorders is controversial¹⁷. Some authors showed that BMC can migrate to a damaged kidney and give rise to proximal tubular cells¹⁸, podocytes¹⁹ and other glomerular cells²⁰, and reverse renal dysfunction¹⁸ or treat a genetic kidney disease such as Alport's syndrome²¹. However, other authors deny the possibility that renal cells can derive from

transplanted bone marrow. One study concluded that intrarenal stem cells but not bone marrow-derived cells are responsible for the regeneration of kidney tissue after ischemic injury and injection of BMC does not make any significant contribution to functional or structural recovery ²². A second study showed that 99% of the BMC-derived cells engrafted in the kidney were leukocytes ²³. In the mouse model of cystinosis, our data demonstrate that in the context of chronic and progressive renal damage, BMC-derived cells can efficiently engraft in the kidney tissue compartment, lead to a significant decrease in cystine content and prevent progression of kidney dysfunction. Indeed, 4 months post-transplantation, 13% of the total renal cells as determined by qPCR (Figure 6B) were derived from the infused wildtype BMC expressing functional *Ctns*. These BMC-derived cells were predominately non-lymphoid lineage interstitial cells but also co-localized with distal and proximal tubular, glomerular and endothelial cells. Moreover, the treated mice exhibited normal serum urea and creatinine levels in contrast to control mice treated with *Ctns*^{-/-} BMC. The renal disease in children with cystinosis starts as a proximal tubulopathy before one year of age, and then evolves to a progressive loss of glomerular function ⁵. Cystine crystals are not abundant in the kidney and are mostly observed in interstitial cells, occasionally in glomerular cells and rarely in tubular cells ^{24,25}. *Ctns*^{-/-} mice develop an incomplete renal disease, but like the human patients, cystine crystals accumulate progressively within interstitial cells ¹³. Thus, BMC-derived interstitial cells in our transplanted mice may have a significant positive effect on the progression of the underlying kidney disease.

On the other hand, MSC did not integrate efficiently within the kidney in our model. Nonetheless, MSC transplantation led to some improvement in renal function

compared to control *Ctns*^{-/-} mice transplanted with *Ctns*^{-/-} BMC. However, after an initial decrease in cystine content at 2 months, cystine levels increased thereafter. In the literature the potential for MSC transplantation to improve kidney failure remains controversial. Several studies showed that in the setting of renal injury, transplanted MSC can generate mesangial and tubular epithelial cells²⁶ and restore renal structure and function^{27,28}. Others showed that MSC injections do not prevent Alport's syndrome in COL4A3-deficient mice and MSC do not differentiate into renal cells²⁹. The protective effects of MSC seem to be due to a paracrine effect of these cells by secretion of growth factors such as VEGF and TGF-β1 rather than cellular differentiation^{30,31}. This mechanism could explain the initial improvement we observed in the *Ctns*^{-/-} mice.

We evaluated the engraftment of BMC-derived cells in multiple tissues based on three metrics: GFP-positive cells identified by confocal microscopy, qPCR for *Ctns* expression and cystine content determined by mass spectrometry. The results by all these metrics showed high levels of engraftment in eye, brain, muscle, liver, spleen and heart. The nature of cystinosis as a clinical entity is a progressive dysfunction of multiple organs caused by the accumulation of cystine in the tissues and thus, the findings here underline the potential utility of BMC transplantation for this genetic disease. Of particular importance is that while cystine levels continued to increase in the *Ctns*^{-/-} mice as a function of time, our data demonstrated that successful transplantation of wildtype BMC reversed this accumulation.

In patients, corneal cystine crystals appear from the first decade of life resulting in photophobia and visual impairment⁴. Cystine crystals are found first in the periphery of the cornea, and then in the center³². *Ctns*^{-/-} mice demonstrate similar ocular anomalies

than patients^{13,33}, and cystine crystals are also first found at the periphery of the cornea. In addition to the decreased cystine content, BMC transplantation led to a significant decrease in the number of mice with corneal cystine crystals (43% WT BMC vs. 86% of *Ctns*^{-/-} BMC; $P < 0.05$). In the third decade of life, patients with cystinosis exhibit a deterioration of the central nervous system characterized by mental deterioration, impaired cerebellar function, pyramidal signs, ischemic lesions and severe impairment in visual short-term memory⁴. Middle-aged *Ctns*^{-/-} mice also present with behavioral anomalies and spatial and working memory deficits that correlate with cystine accumulation in the brain^{13,34}. In the present study, we demonstrated *Ctns* expressing BMC-derived cells in the brain, differentiated into or fused with endothelial or smooth muscle cells as well as some glial-like cells. For another LSD, metachromatic leukodystrophy, partial³⁵ or total³⁶ correction was observed after BMC transplantation in the mouse model. BMC-derived cells repopulated the central nervous system microglia³⁶. For α -mannosidosis, functional enzyme was present in neurons, glial cells and cells associated with blood vessels after BMC transplantation in kittens lacking α -mannosidase³⁷.

Without cysteamine, cystinotic patients develop myopathy with atrophy and progressive distal extremity weakness as well as progressive oromotor dysfunction including dysphagia⁴. Cystine crystals were observed in fibroblastic cells adjacent to muscle fibers and within perimysial collagen fibrils and muscle necrosis was also observed³⁸. The *Ctns*^{-/-} mice also present with muscular impairment associated with cystine crystals located in interstitial cells and myocyte necrosis¹³. Cardiomyopathy can be a late complication in cystinosis⁴ and one autopsy revealed the presence of cystine

crystals in interstitial cardiac histiocytes and one myocardial cell³⁹. Similarly, crystals were abundant in interstitial cells of *Ctns*^{-/-} mice heart but not in myocytes¹³. In our data, *Ctns*-expressing BMC-derived cells in heart and skeletal muscle were mostly interstitial, though some GFP-positive muscle fibers were present. The spleen was the organ in which we found the most abundant amount of *Ctns*-expressing BMC-derived cells. Curiously most of these cells were not of lymphoid lineage, but rather part of the reticulo-endothelial system. Some patients require a splenectomy due to accumulation of cystine crystals in endothelial cells and macrophages in the spleen⁴⁰. Finally, cystine crystals are found in Kupffer cells in the liver of patients⁴⁰. Our results show that *Ctns*-expressing BMC-derived cells in the liver were essentially all Kupffer cells.

Only engraftment of bone marrow cells producing a functional *Ctns* was able to reverse the disease process and reduce tissue cystine levels in our model as *Ctns*^{-/-} mice transplanted with *Ctns*^{-/-} BMC still accumulated cystine and developed kidney dysfunction. The fact that lethally irradiated wildtype mice exhibited few transplanted BMC-derived cells in the tissues, as shown by confocal microscopy for GFP-positive cells and IVIS imaging for luciferase-expressing cells, proves that the extensive colonization of *Ctns*^{-/-} mice by wildtype BMC-derived cells is specifically due to the impact of cystinosis. The few BMC-derived cells observed in wildtype mice might be myeloid and lymphoid lineage fusion hybrids that can occur after lethally irradiation of mice⁴¹. In contrast, *Ctns*^{-/-} mice exhibited abundant BMC-derived cells (e.g. GFP-positive) that co-localized with tissue-specific cell phenotypes and the studies of luciferase BMC-derived cells in live animals confirmed the increase in engraftment over time. Moreover, most of these cells were not from the lymphoid lineage (specifically, not

macrophages) even in the spleen, but were part of the intrinsic structure of the organ. Tissue engraftment of bone marrow-derived cells can occur through cell differentiation or cell fusion⁴². For instance, bone marrow cells can give rise to endothelial, smooth muscle reticuloendothelial, and Kupffer cells through differentiation^{43,44,45} and skeletal muscle through fusion⁴⁶. However, this field is still controversial^{47,48} and in our case the mechanism remains to be established.

Taken together, the literature on cystinosis and our data indicate that *Ctns* expressing BMC replace or fuse with cells that accumulate the most cystine crystals in each tissue. Thus, BMC transplantation creates a reservoir of healthy cells that migrate to the targeted organ as a function of progressive cellular injury and may replace or fuse with the cells accumulating the highest levels of cystine, many of which are interstitial and reticuloendothelial cells. Consistent with this conclusion, Hippert et al. depleted 75% of the liver cystine content in *Ctns*^{-/-} mice by chemically depleting Kupffer cells representing less than 10% of the total cells in the liver¹⁴. It is also interesting to note that the addition of the *CTNS* gene to *Ctns*^{-/-} hepatocytes in culture resulted in a significant decrease in cystine levels¹⁴. We have confirmed these experiments using *Ctns*^{-/-} fibroblasts (data not shown). In sum, these data add additional support to the conclusion that there is a direct relationship between expression of a functional protein and the reduction in cystine levels.

Cystinosin is a transmembrane protein localized to the intracellular lysosomal membrane. Thus, cells lacking *Ctns* cannot recapture the normal protein from transplanted wildtype cells even in close proximity. In contrast, in Hurler syndrome normal enzyme can be secreted by BMC-tissue engrafted cells and taken up by adjacent

host cells. Indeed, in a murine model of Hurler syndrome treated by transplantation of retroviral-transduced bone marrow cells, tissue engraftment of transgene-positive cells was low, primarily limited to spleen and liver. Nonetheless, glycosaminoglycan levels decreased in all the tissues tested and that effect was explained by uptake of the secreted enzyme by adjacent cells^{49,50}. In contrast, in our studies, the mechanism underlying the decrease of cystine in all tissues involves the localization of cells expressing the functional gene and thus, is correlated with the abundant engraftment of BMC-derived cells. Therefore, BMC transplantation for cystinosis is an example where therapeutic efficacy requires the local integration of cells with the functional protein rather than local delivery of a missing enzyme like many LSD.

Hematopoietic stem cell transplantation, modeled in mice by purification of Sca1⁺ HSC, has the same therapeutic effects as whole bone marrow cell transplantation in the mouse model of cystinosis including high levels of tissue engraftment and significant decreases in cystine content. This is important because human HSC (CD34⁺) are readily isolated from peripheral blood after growth factor-mediated mobilization (i.e. GM-CSF) and this population is significantly enriched for the true HSC. Moreover, future *ex vivo* gene delivery to introduce a functional *Ctns* gene will be more efficient with purified HSC than with whole BMC.

This work represents the first step towards a clinical trial of using bone marrow cell transplantation as a therapy for cystinosis. This disease, like many lysosomal storage disorders, is a slowly progressive process that represents an ongoing cystine accumulation leading downstream to cell stress, cell death, tissue injury and eventually to organ dysfunction including kidney failure, blindness and progressive myopathy. The

permanent engraftment of bone marrow cells expressing a fully functional *CTNS* gene would provide a continuous source of healthy cells that could traffic to different tissue compartments where cells are stressed or dying from cystine accumulation. We have demonstrated the high efficiency of this strategy in the cystinosis model as determined objectively by significant levels of bone marrow-derived cell engraftment in multiple tissue compartments correlated with improvements in measured cystine content and renal function. These results suggest that bone marrow cell or hematopoietic stem cell transplantation is particularly suitable for the chronic and progressive injury characteristic of cystinosis and potentially other lysosomal storage disorders in which mutations of intracellular and transmembrane proteins are involved.

Acknowledgments

We acknowledge the expert assistance of Dr. Marie-Claire Gubler for the kidney histology. This work was funded by the Cystinosis Research Foundation and the Molly Baber Research Fund. No support for this work was derived from any commercial source and the authors have no direct financial interest in any aspect of the manuscript.

Authorship

K.S., F.H., M.T. and S.C. performed research and analyzed data. S.C. and D.S. designed the project and wrote the manuscript. J.J. and J.S., ophthalmologist, performed the eye analysis. S.R., neuropathologist, contributed to the brain analysis.

References

1. Town M, Jean G, Cherqui S, et al. A novel gene encoding an integral membrane protein is mutated in nephropathic cystinosis. *Nat Genet.* 1998;18:319-324.
2. Cherqui S, Kalatzis V, Trugnan G, Antignac C. The targeting of cystinosin to the lysosomal membrane requires a tyrosine-based signal and a novel sorting motif. *J Biol Chem.* 2001;276:13314-13321.
3. Kalatzis V, Cherqui S, Antignac C, Gasnier B. Cystinosin, the protein defective in cystinosis, is a H(+)-driven lysosomal cystine transporter. *Embo J.* 2001;20:5940-5949.
4. Nesterova G, Gahl W. Nephropathic cystinosis: late complications of a multisystemic disease. *Pediatr Nephrol.* 2007.
5. Gahl WA, Thoene JG, Schneider JA. Cystinosis. *N Engl J Med.* 2002;347:111-121.
6. Pastores GM, Barnett NL. Current and emerging therapies for the lysosomal storage disorders. *Expert Opin Emerg Drugs.* 2005;10:891-902.
7. Kleta R, Gahl WA. Pharmacological treatment of nephropathic cystinosis with cysteamine. *Expert Opin Pharmacother.* 2004;5:2255-2262.
8. Krivit W. Allogeneic stem cell transplantation for the treatment of lysosomal and peroxisomal metabolic diseases. *Springer Semin Immunopathol.* 2004;26:119-132.
9. Peters C, Steward CG. Hematopoietic cell transplantation for inherited metabolic diseases: an overview of outcomes and practice guidelines. *Bone Marrow Transplant.* 2003;31:229-239.
10. Braunlin EA, Rose AG, Hopwood JJ, Candel RD, Krivit W. Coronary artery patency following long-term successful engraftment 14 years after bone marrow transplantation in the Hurler syndrome. *Am J Cardiol.* 2001;88:1075-1077.
11. Peters C, Shapiro EG, Anderson J, et al. Hurler syndrome: II. Outcome of HLA-genotypically identical sibling and HLA-haploidentical related donor bone marrow transplantation in fifty-four children. The Storage Disease Collaborative Study Group. *Blood.* 1998;91:2601-2608.
12. Staba SL, Escolar ML, Poe M, et al. Cord-blood transplants from unrelated donors in patients with Hurler's syndrome. *N Engl J Med.* 2004;350:1960-1969.
13. Cherqui S, Sevin C, Hamard G, et al. Intralysosomal cystine accumulation in mice lacking cystinosin, the protein defective in cystinosis. *Molecular & Cellular Biology.* 2002;22:7622-7632.
14. Hippert C, Dubois G, Morin C, et al. Gene Transfer May Be Preventive But Not Curative for a Lysosomal Transport Disorder. *Mol Ther.* 2008;16:1372-1381.
15. Meirelles Lda S, Nardi NB. Murine marrow-derived mesenchymal stem cell: isolation, in vitro expansion, and characterization. *Br J Haematol.* 2003;123:702-711.
16. Schneider JA. Approval of cysteamine for patients with cystinosis. *Pediatr Nephrol.* 1995;9:254.
17. Cantley LG. Adult stem cells in the repair of the injured renal tubule. *Nat Clin Pract Nephrol.* 2005;1:22-32.
18. Kale S, Karihaloo A, Clark PR, Kashgarian M, Krause DS, Cantley LG. Bone marrow stem cells contribute to repair of the ischemically injured renal tubule. *Journal of Clinical Investigation.* 2003;112:42-49.

19. Poulson R, Forbes SJ, Hodivala-Dilke K, et al. Bone marrow contributes to renal parenchymal turnover and regeneration. *Journal of Pathology*. 2001;195:229-235.
20. Ito T, Suzuki A, Imai E, Okabe M, Hori M. Bone marrow is a reservoir of repopulating mesangial cells during glomerular remodeling. *Journal of the American Society of Nephrology*. 2001;12:2625-2635.
21. Sugimoto H, Mundel TM, Sund M, Xie L, Cosgrove D, Kalluri R. Bone-marrow-derived stem cells repair basement membrane collagen defects and reverse genetic kidney disease. *Proc Natl Acad Sci U S A*. 2006;103:7321-7326.
22. Lin F, Moran A, Igarashi P. Intrarenal cells, not bone marrow-derived cells, are the major source for regeneration in postischemic kidney. *J Clin Invest*. 2005;115:1756-1764.
23. Duffield JS, Park KM, Hsiao LL, et al. Restoration of tubular epithelial cells during repair of the postischemic kidney occurs independently of bone marrow-derived stem cells. *J Clin Invest*. 2005;115:1743-1755.
24. Mahoney CP, Striker GE. Early development of the renal lesions in infantile cystinosis. *Pediatr Nephrol*. 2000;15:50-56.
25. Spear GS, Gubler MC, Habib R, Broyer M. Renal allografts in cystinosis and mesangial demography. *Clin Nephrol*. 1989;32:256-261.
26. Yokoo T, Sakurai T, Ohashi T, Kawamura T. Stem cell gene therapy for chronic renal failure. *Current Gene Therapy*. 2003;3:387-394.
27. Herrera MB, Bussolati B, Bruno S, Fonsato V, Romanazzi GM, Camussi G. Mesenchymal stem cells contribute to the renal repair of acute tubular epithelial injury. *Int J Mol Med*. 2004;14:1035-1041.
28. Morigi M, Imberti B, Zoja C, et al. Mesenchymal stem cells are renotropic, helping to repair the kidney and improve function in acute renal failure. *J Am Soc Nephrol*. 2004;15:1794-1804.
29. Ninichuk V, Gross O, Segerer S, et al. Multipotent mesenchymal stem cells reduce interstitial fibrosis but do not delay progression of chronic kidney disease in collagen4A3-deficient mice. *Kidney Int*. 2006;70:121-129.
30. Kunter U, Rong S, Djuric Z, et al. Transplanted mesenchymal stem cells accelerate glomerular healing in experimental glomerulonephritis. *J Am Soc Nephrol*. 2006;17:2202-2212.
31. Togel F, Cohen A, Zhang P, Yang Y, Hu Z, Westenfelder C. Autologous and allogeneic marrow stromal cells are safe and effective for the treatment of acute kidney injury. *Stem Cells Dev*. 2008.
32. Melles RB, Schneider JA, Rao NA, Katz B. Spatial and temporal sequence of corneal crystal deposition in nephropathic cystinosis. *Am J Ophthalmol*. 1987;104:598-604.
33. Kalatzis V, Serratrice N, Hippert C, et al. The ocular anomalies in a cystinosis animal model mimic disease pathogenesis. *Pediatr Res*. 2007;62:156-162.
34. Maurice T, Hippert C, Serratrice N, et al. Cystine accumulation in the CNS results in severe age-related memory deficits. *Neurobiol Aging*. 2007.
35. Matzner U, Hartmann D, Lullmann-Rauch R, et al. Bone marrow stem cell-based gene transfer in a mouse model for metachromatic leukodystrophy: effects on visceral and nervous system disease manifestations. *Gene Ther*. 2002;9:53-63.

36. Biffi A, De Palma M, Quattrini A, et al. Correction of metachromatic leukodystrophy in the mouse model by transplantation of genetically modified hematopoietic stem cells. *J Clin Invest*. 2004;113:1118-1129.
37. Walkley SU, Thrall MA, Dobrenis K, et al. Bone marrow transplantation corrects the enzyme defect in neurons of the central nervous system in a lysosomal storage disease. *Proc Natl Acad Sci U S A*. 1994;91:2970-2974.
38. Charnas LR, Luciano CA, Dalakas M, et al. Distal vacuolar myopathy in nephropathic cystinosis. *Ann Neurol*. 1994;35:181-188.
39. Dixit MP, Greifer I. Nephropathic cystinosis associated with cardiomyopathy: a 27-year clinical follow-up. *BMC Nephrol*. 2002;3:8.
40. Gagnadoux MF, Tete MJ, Guest G, Arsan A, Broyer M. Hepatosplenic disorders in nephropathic cystinosis. In: Broyer M, ed. *Cystinosis* (ed Paris: Elsevier); 1999:70-74.
41. Nygren JM, Liuba K, Breitbart M, et al. Myeloid and lymphoid contribution to non-haematopoietic lineages through irradiation-induced heterotypic cell fusion. *Nat Cell Biol*. 2008;10:584-592.
42. Pessina A, Gribaldo L. The key role of adult stem cells: therapeutic perspectives. *Curr Med Res Opin*. 2006;22:2287-2300.
43. Bailey AS, Willenbring H, Jiang S, et al. Myeloid lineage progenitors give rise to vascular endothelium. *Proc Natl Acad Sci U S A*. 2006;103:13156-13161.
44. Tanaka K, Sata M. Contribution of circulating vascular progenitors in lesion formation and vascular healing: lessons from animal models. *Curr Opin Lipidol*. 2008;19:498-504.
45. Klein I, Cornejo JC, Polakos NK, et al. Kupffer cell heterogeneity: functional properties of bone marrow derived and sessile hepatic macrophages. *Blood*. 2007;110:4077-4085.
46. Sherwood RI, Christensen JL, Weissman IL, Wagers AJ. Determinants of skeletal muscle contributions from circulating cells, bone marrow cells, and hematopoietic stem cells. *Stem Cells*. 2004;22:1292-1304.
47. Kashofer K, Bonnet D. Gene therapy progress and prospects: stem cell plasticity. *Gene Ther*. 2005;12:1229-1234.
48. Quesenberry PJ, Dooner G, Colvin G, Abedi M. Stem cell biology and the plasticity polemic. *Exp Hematol*. 2005;33:389-394.
49. Di Domenico C, Villani GR, Di Napoli D, et al. Gene therapy for a mucopolysaccharidosis type I murine model with lentiviral-IDUA vector. *Hum Gene Ther*. 2005;16:81-90.
50. Zheng Y, Rozengurt N, Ryazantsev S, Kohn DB, Satake N, Neufeld EF. Treatment of the mouse model of mucopolysaccharidosis I with retrovirally transduced bone marrow. *Mol Genet Metab*. 2003;79:233-244.

Table 1: Serum and urine analyses for renal function.

n = 12 per group	Wildtype Controls [§]	Ctns ^{-/-} Controls*	WT BMC**	Ctns ^{-/-} BMC [†]	WT MSC [‡]
serum					
Creatinine (mg/dL)	0.34 + 0.06	0.49 + 0.30 ^{a,b}	0.35 + 0.07	0.43 + 0.10 ^{a,b}	0.38 + 0.11
Creatinine clearance (μl/min)	79.40 + 74.24	32.28 + 42.58	65.65 + 72.34	43.04 + 34.46	85.35 + 64.60
Urea (mg/dL)	36.54 + 1.55	56.92 + 18.41 ^{a,b}	23.83 + 19.62	74.95 + 17.32 ^{a,b}	41.98 + 4.85 ^b
Phosphate (mg/dL)	18.31 + 3.06	23.09 + 4.70 ^b	10.95 + 6.82	10.57 + 7.53	11.86 + 6.35
Alkaline Phosphatase (IU/L)	60.54 + 23.57	67.35 + 26.75	75.77 + 21.10	67.76 + 18.10	55.73 + 16.20
urine					
Phosphate (μmol/24h)	3.50 + 2.29	11.00 + 4.90 ^{a,b}	3.75 + 2.35	2.70 + 2.87	5.11 + 3.29
Protein (mg/24h)	10.16 + 6.21	17.28 + 8.45	9.37 + 6.91	8.35 + 4.35	11.43 + 7.08

[§]**Wildtype Controls** = non-treated wildtype C57BL/6 mice

***Ctns^{-/-} Controls** = non-treated C57BL/6 Ctns^{-/-} mice

****WT BMC** = Ctns^{-/-} mice treated with wildtype BMC

[†]**Ctns^{-/-} BMC** = Ctns^{-/-} mice treated with Ctns^{-/-} BMSC

[‡]**WT MSC** = Ctns^{-/-} mice treated with wildtype MSC

^aP<0.05 compared to wildtype mice

^bP<0.05 compared to Ctns^{-/-} WT BMSC

Table 2: Cystine content* in the different tissues of treated and control mice at 2 and 4 months post-transplant.

	2 months (n = 3 animals per group)				4 months (n = 12 animals per group)			
	Wildtype Controls	Ctns ^{-/-} BMC	WT BMC	WT MSC	Wildtype Controls	Ctns ^{-/-} BMC	WT BMC	WT MSC
Brain	0.02 + 0.00	0.70 + 0.15	0.61 + 0.29	0.75 + 0.28	0.02 + 0.00	1.38 + 0.45	0.59 + 0.32 ^a	0.62 + 0.32
Eye	0.07 + 0.20	20 + 11	18 + 11	27 + 4	0.1 + 0.02	45 + 12	13 + 8 ^a	36 + 9
Heart	0.17 + 0.10	25 + 7	23 + 16	10 + 1 ^a	0.08 + 0.10	61 + 15	11 + 8 ^a	25 + 9 ^a
Kidney	0.18 + 0.05	76 + 16	135 + 12	45 + 24	0.25 + 0.06	116 + 63	35 + 34 ^a	59 + 34 ⁱ
Liver	0.02 + 0.01	57 + 3	6 + 0.2 ^a	62 + 23	0.02 + 0.02	62 + 19	3 + 1 ^a	51 + 15
Muscle	0.23 + 0.13	17 + 7	15 + 2	10 + 0.7	0.07 + 0.20	30 + 11	10 + 6 ^a	22 + 4
Spleen	0.06 + 0.04	91 + 39	38 + 5 ^a	124 + 35	0.12 + 0.03	160 + 50	21 + 19 ^a	95 + 17 ⁱ

* nmol half-cystine/mg protein

^a P<0.05 compared to mice treated with Ctns^{-/-} BMC

Table 3: *Ctns* expression* in the different tissues of treated and control mice at 2 and 4 months post-transplant.

	2 months (n = 3 animals per group)				4 months (n = 12 animals per group)			
	Wildtype Controls	<i>Ctns</i> ^{-/-} BMC	WT BMC	WT MSC	Wildtype Controls	<i>Ctns</i> ^{-/-} BMC	WT BMC	WT MSC
Brain	40352 + 41063	ND**	694 + 842	2 + 2	8362 + 3814	ND	520 + 151	1 + 1
Eye	124553 + 17116	ND	14722 + 20816	12 + 13	52942 + 35772	ND	8226 + 3361	2 + 2
Heart	44510 + 15675	ND	3865 + 5415	2 + 1	27089 + 13649	ND	3359 + 2761	1 + 1
Kidney	304504 + 95560	ND	6569 + 1749	31 + 54	47709 + 26694	ND	7071 + 10917	3 + 6
Liver	38616 + 32898	ND	674 + 319	15 + 23	180281 + 15749	ND	19201 + 12787	1 + 0
Muscle	36233 + 15457	ND	342 + 119	ND	28148 + 12428	ND	1617 + 1223	3 + 4
Spleen	185567 + 24855	ND	1375 + 968	3 + 3	136147 + 11703	ND	32555 + 14730	6 + 10

*Relative expression of *Ctns* as18S-normalized fold changes

**ND means Non Detected

Table 4: *Ctns* expression and cystine content in the different tissues of mice treated with Sca1+ HSC compared to wildtype and *Ctns*^{-/-} controls

a- Relative expression of *Ctns* as fold changes*

	Wildtype mice	<i>Ctns</i> ^{-/-} mice	<i>Ctns</i> ^{-/-} mice Sca1+ HSC	Percentage <i>Ctns</i> in Sca1-transplanted vs. wildtype mice
Brain	93381 + 93056	ND**	1940 + 2201	2.1
Eye	780359 + 899835	ND	34532 + 26910	4.4
Heart	204857 + 143183	ND	8725 + 3488	4.3
Kidney	72120 + 36321	ND	6291 + 7818	8.7
Liver	26656 + 21901	ND	3588 + 2558	13.5
Muscle	46125 + 11840	ND	3288 + 2923	7.1
Spleen	19634 + 3603	ND	15218 + 3590	77.5

*18S-normalized fold changes

**ND means Non Detected

b- Cystine content (nmol half-cystine/mg protein)

	Wildtype mice	<i>Ctns</i> ^{-/-} mice	<i>Ctns</i> ^{-/-} mice Sca1+ HSC	Percentage cystine decrease in Sca1-transplanted vs. <i>Ctns</i> ^{-/-} mice
Brain	0.02 + 0.01	1.33 + 0.40	0.57 + 0.13 ^a	57.5
Eye	0.04 + 0.01	47.46 + 14.95	9.25 + 1.33 ^a	80.5
Heart	0.14 + 0.05	58.85 + 14.28	5.48 + 2.33 ^a	90.7
Kidney	0.19 + 0.06	112.85 + 59.72	63.72 + 49.40 ^a	43.5
Liver	0.02 + 0.01	60.21 + 20.58	4.07 + 1.83 ^a	93.2
Muscle	0.22 + 0.10	29.19 + 9.96	6.71 + 1.44 ^a	77.0
Spleen	0.06 + 0.03	168.75 + 52.08	16.76 + 16.69 ^a	90.1

^a*p*<0.05 compared to *Ctns*^{-/-} mice control

Figure legends

Figure 1: Representative images of Z-series confocal microscopy of kidneys.

Transplanted, BMC-derived GFP-positive cells are seen in green. (A, C, E) F-actin intermediate filament staining by Bodipy-Phalloidin (red) and nuclei staining by dapi (blue). (B, D, F) Same picture without Bodipy-Phalloidin to better observe the GFP-positive cells. (A and B) Kidney section of *Ctns*^{-/-} mice treated with *Ctns*^{-/-} BMC; no GFP-positive cells are observed establishing the threshold for GFP detection. These instrument settings were saved and used for all the subsequent imaging. (C and D) Representative kidney section of wildtype mice transplanted with GFP BMC. Few GFP-positive cells are observed. (E and F) Kidney section of *Ctns*^{-/-} mice transplanted with GFP BMC. Abundant GFP-positive BMC-derived cells are evident. Scale bar, 20 μ m.

Figure 2: Representative Z-series confocal microscopy pictures of WT BMC-treated kidneys to demonstrate cell phenotypes.

Transplanted, BMC-derived GFP-positive cells are seen in green. (A) F4/80-positive macrophages are stained in blue and CD45-positive leukocyte lineage cells are stained in red. Few GFP-positive cells are macrophages (white, arrows). (B) Distal tubular staining by Dolichos Biflorus Agglutinin (red). Some GFP-positive cells are co-localized with distal tubular cells (yellow, arrows) (C) Proximal tubular staining by Lotus Tetragonolobus lectin (red). Some GFP-positive cells are co-localized with proximal tubular cells (yellow, arrow) (D) F-actin intermediate filament staining by Bodipy-Phalloidin (red). Some GFP-positive cells are found in the glomeruli (E) Tubular basement membrane staining by Ricinus Communis Agglutinin I (red). Some GFP-

positive cells co-localize with the basal membranes (arrow). (F) Endothelial cell staining with anti-vWF antibody (blue). Some GFP-positive cells are co-localized with endothelial cells (white, arrow). Scale bars, 10 μm except for (B) Scale bar, 50 μm .

Figure 3: Representative Z-series confocal microscopy pictures of the eyes and brains of mice treated with wildtype BMC.

Transplanted, BMC-derived GFP-positive cells are seen in green (A-D) Eye. Bodipy phalloidin is seen in red. Scale bars, 50 μm . GFP-positive cells were observed in the corneal stroma (A) and adjacent to the basal cells of the corneal epithelium (B). Heavy perivascular infiltrates around the limbus were also observed (C). Corneal cystine crystals (D, arrow). (E-H) Brain, Scale bars, 10 μm . The majority of the GFP-positive cells were observed in association with blood vessels. Small round cells were observed in the lumen, many appearing to be attached to the endothelium. Large flat cells were either fused with or differentiated into smooth muscle cells co-localizing with f-actin seen in red (E, yellow, arrow) or endothelial cells co-localizing with vWF seen in blue (F, white, arrow). A few GFP-positive cells were macrophages (G, white, arrow). Some were glial cells co-localizing with glial fibrillary acidic protein staining seen in red (H, yellow, arrow).

Figure 4: Representative Z-series confocal microscopy pictures of the muscle and spleen of mice treated with wildtype BMC.

Transplanted, BMC-derived GFP-positive cells are seen in green (A, D), F-actin intermediate filament staining by Bodipy-phalloidin is seen in red (B, E) and

colocalization of both stains is shown in the last panels (**C, F**). Muscle (**A-C**). Nuclei stained by Dapi are blue. Some GFP-positive cells are interstitial and some are differentiated or fused with muscle fibers as shown by the co-localization of GFP-positive with muscle fibers (**C**). Spleen (**D-F**). Most of the GFP-positive cells in the spleen are part of the reticulo-endothelium as determined by co-localization with vWF (blue) and f-actin staining (**F**). Scale bars, 10 μ m.

Figure 5: Tissue cystine content in *Ctns*^{-/-} mice treated with WT BMC compared to *Ctns*^{-/-} mice treated with *Ctns*^{-/-} BMC.

(**A**) Cystine content at 2 and 4 months in *Ctns*^{-/-} mice. Cystine levels increase with time after transplantation of *Ctns*^{-/-} BMC (\blackstar). In contrast, cystine content decreases in time after therapy with WT BMC (\blackstar). (**B**) Table of percent decrease in cystine content of *Ctns*^{-/-} mice treated with WT BMC compared to *Ctns*^{-/-} mice treated *Ctns*^{-/-} BMC.

Figure 6: In vivo luciferase imaging and quantitative *Ctns* expression in *Ctns*^{-/-} mice treated with WT BMC as a function of time.

BMC isolated from luciferase transgenic mice were transplanted into lethally irradiated *Ctns*^{-/-} mice (upper panel) and wildtype mice (lower panel). These are representative pictures taken in live animals with the IVIS imaging system after luciferin injection at 2, 3 and 4 months. The luminescence signal intensities were quantified and are represented in the matching histograms. (**B**) Percent of *Ctns* expression in *Ctns*^{-/-} mice treated with WT BMC compared with wildtype mice. The results represent the number of *Ctns* gene copies determined by RT-qPCR as a ratio of the results shown in Table 3 for BMC-treated *Ctns*^{-/-} mice divided by the results for wildtype control mice.

Figure 1

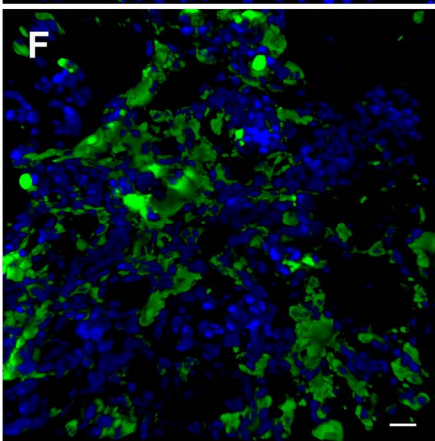
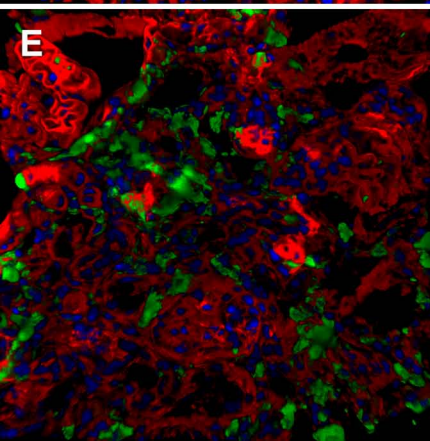
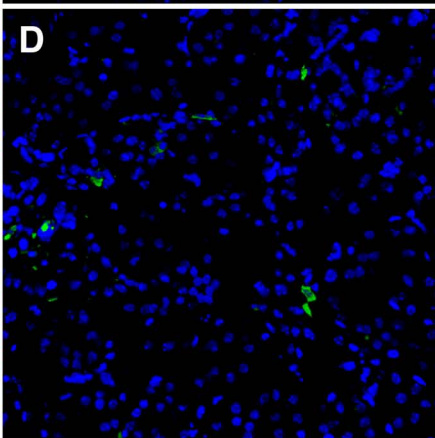
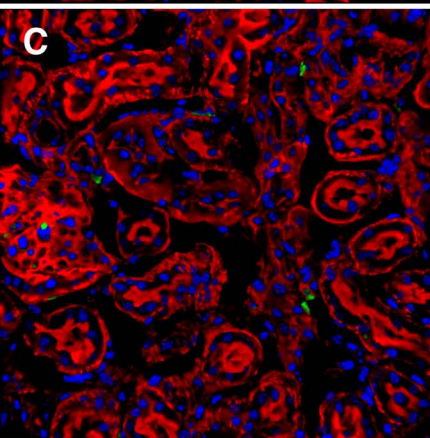
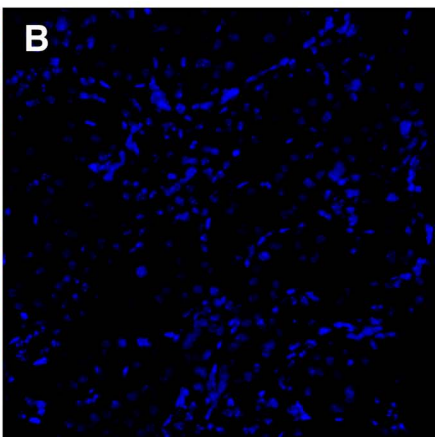
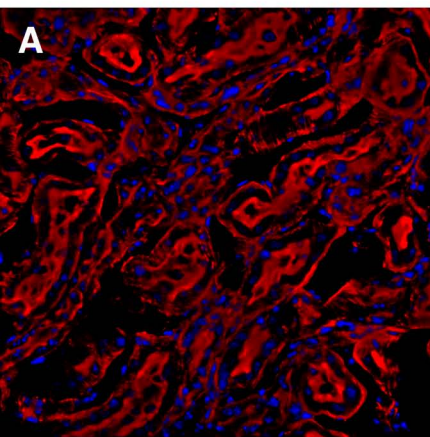


Figure 2

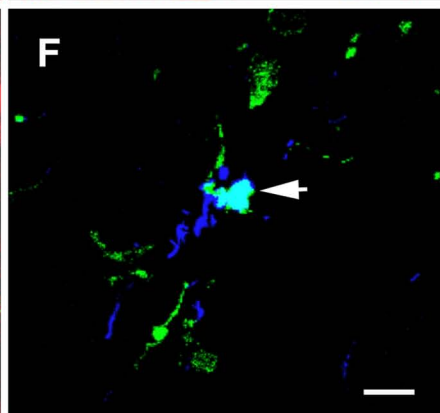
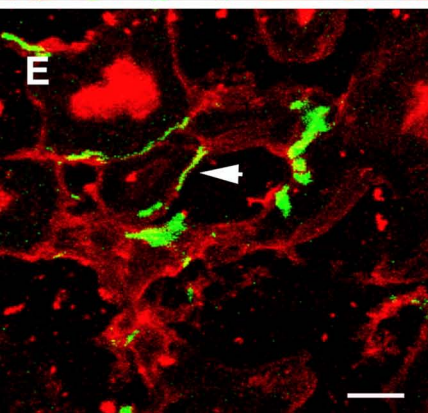
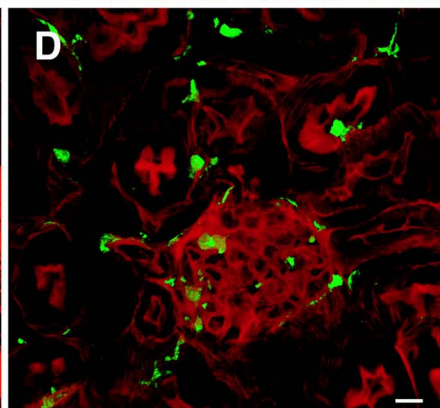
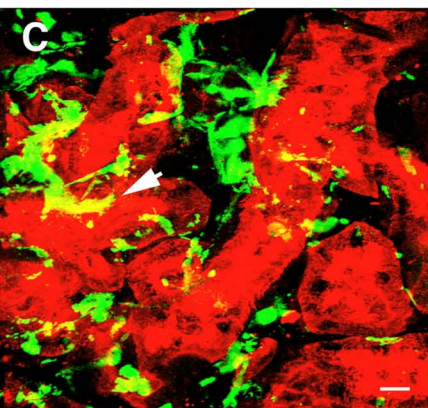
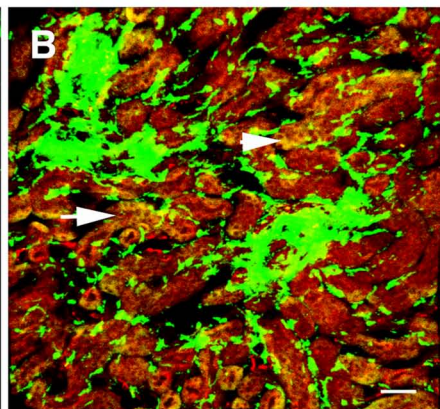
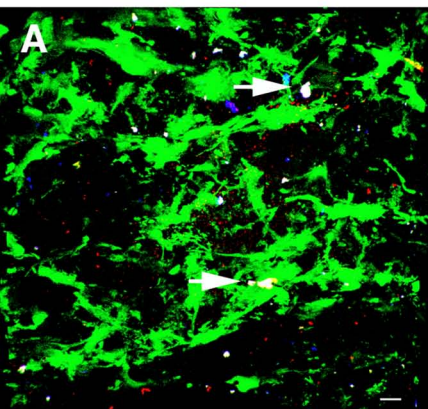
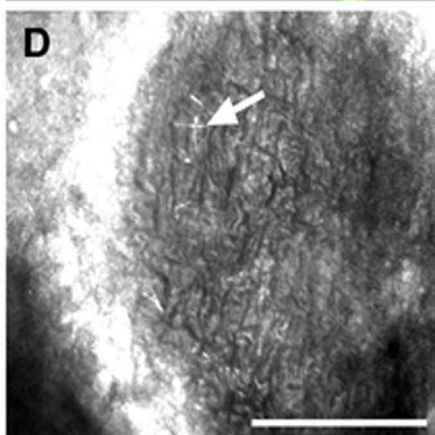
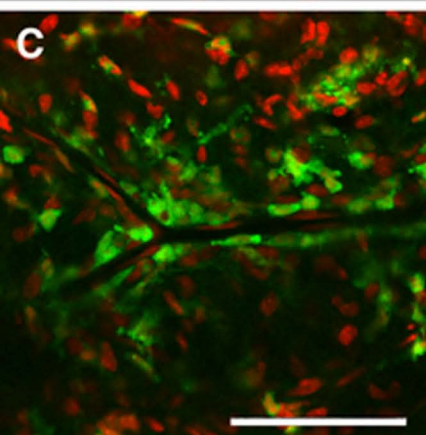
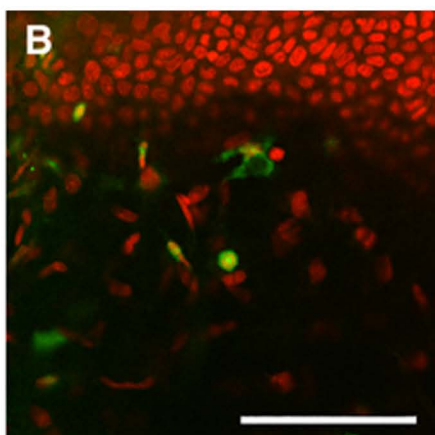
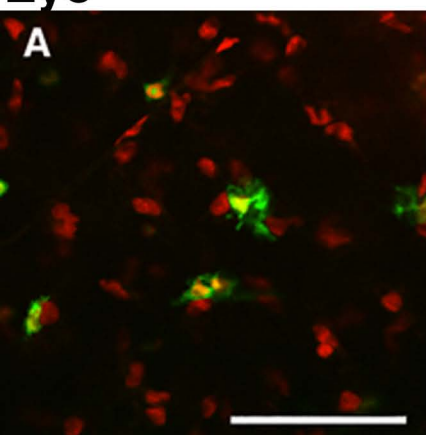


Figure 3
Eye



Brain

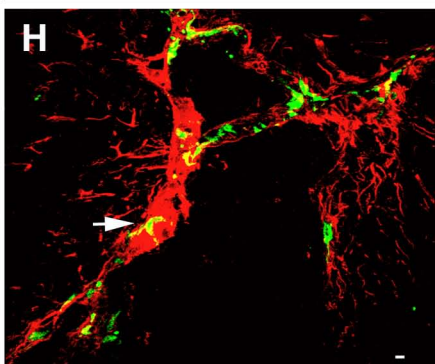
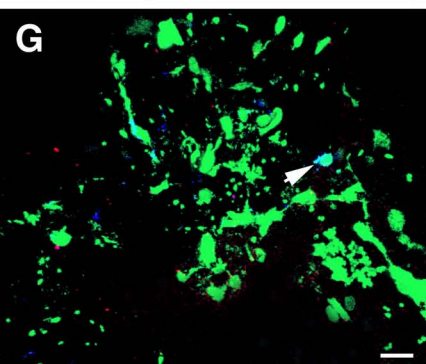
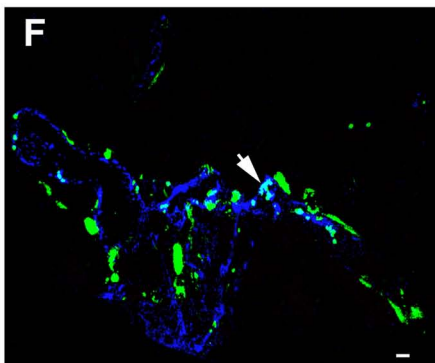
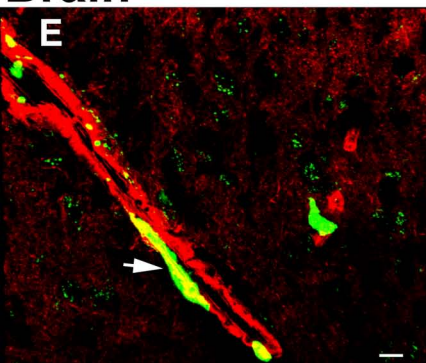


Figure 4

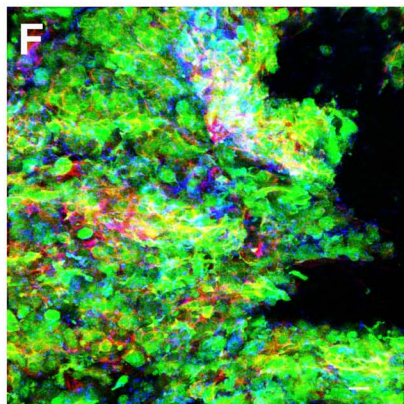
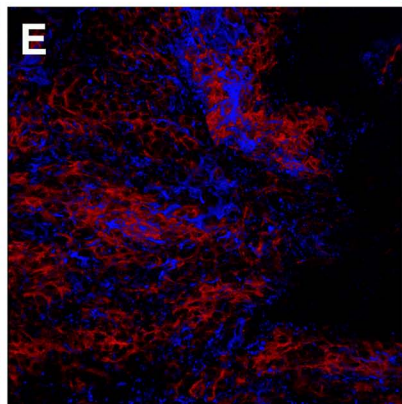
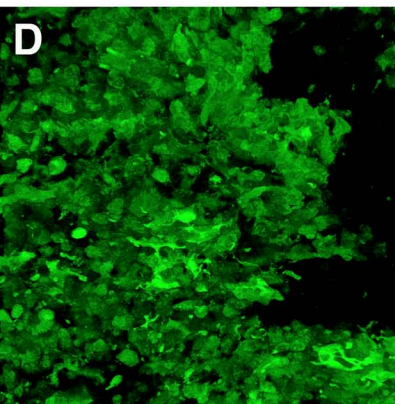
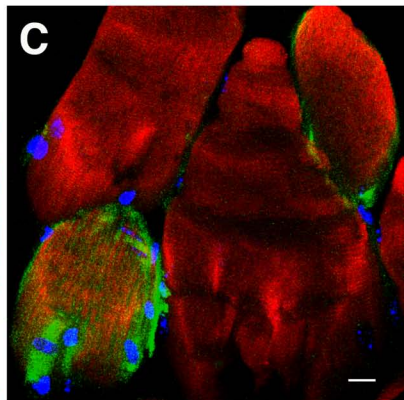
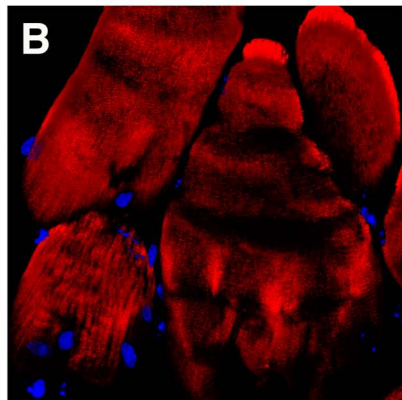
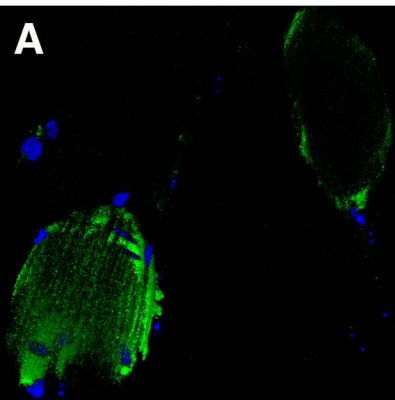
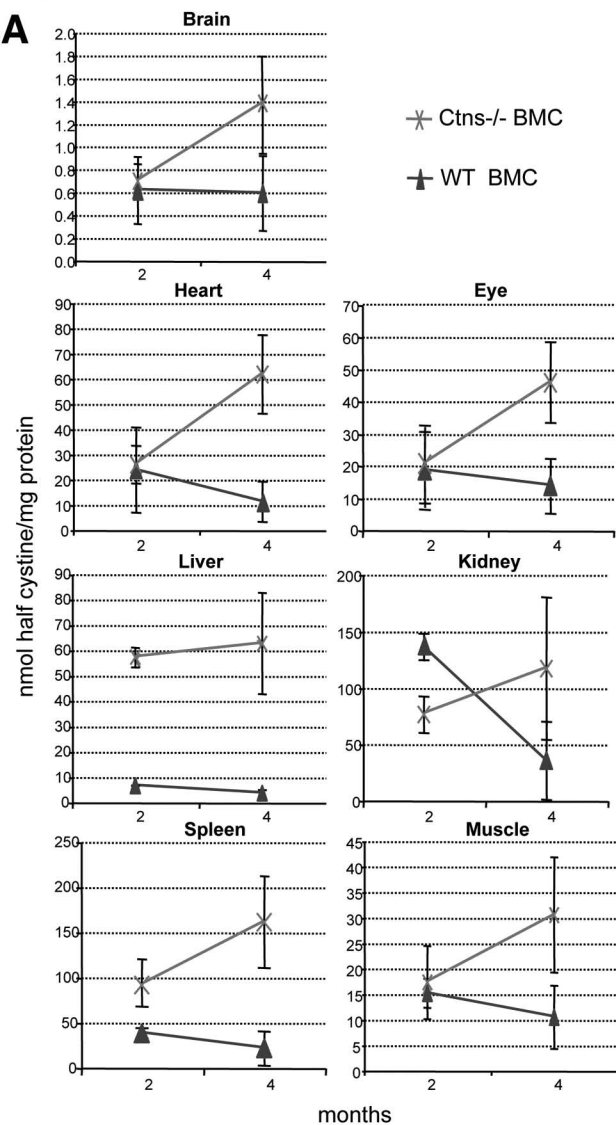


Figure 5

A

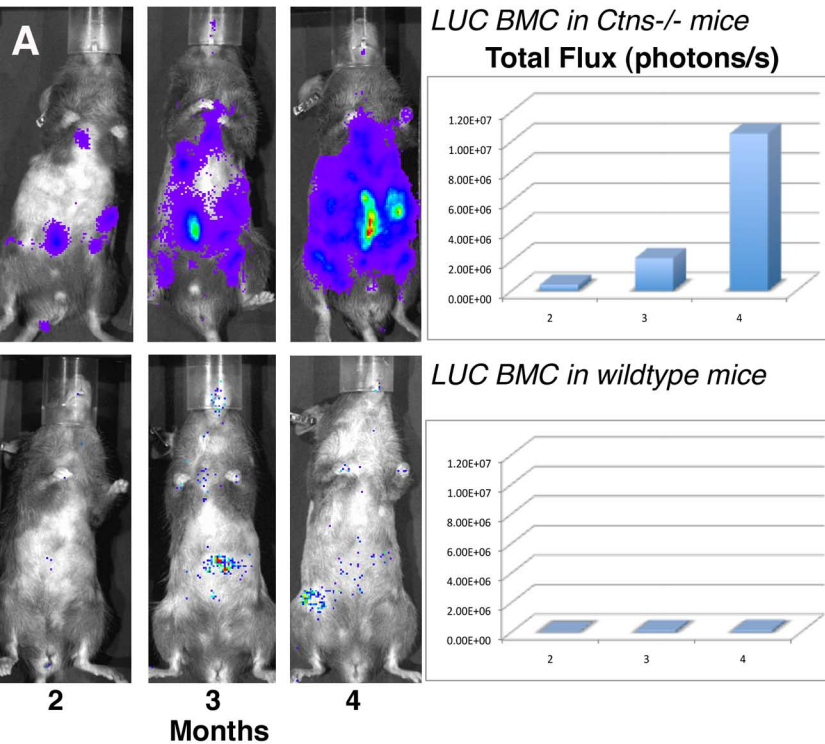


B

	Percent decrease in cystine*	
	2 months	4 months
Brain	11.6	57.3
Eye	9.5	70.4
Heart	8.4	81.9
Kidney	-35.7	70
Liver	88.4	94.4
Muscle	12.2	65.6
Spleen	58.2	86.8

*Percent decrease in cystine content in Ctns^{-/-} mice treated with WT BMC compared to Ctns^{-/-} mice treated with Ctns^{-/-} BMC.

Figure 6



B

	Percent of <i>Ctns</i> expression*	
	2 months	4 months
Brain	1.7	5.9
Eye	10.6	13.4
Heart	8.0	11.0
Kidney	2.1	12.9
Liver	1.7	9.6
Muscle	0.9	5.4
Spleen	0.7	19.3

*Percent of *Ctns* expression in *Ctns^{-/-}* mice treated with WT BMC compared to wildtype mice.